

MAGNETIC RESONANCE IMAGING OF THE KNEE

CURRENT TECHNIQUES AND SPECTRUM OF DISEASE

BY A. JAY KHANNA, MD, ANDREW J. COSGAREA, MD, MICHAEL A. MONT, MD, BRETT M. ANDRES, MD,
BENJAMIN G. DOMB, MD, PETER J. EVANS, MD, DAVID A. BLUEMKE, MD, PHD, AND FRANK J. FRASSICA, MD

Magnetic resonance imaging is an excellent modality for visualizing pathological processes of the knee joint. It allows high-resolution imaging not only of the osseous structures of the knee but, more importantly, also of the soft-tissue structures, including the menisci and ligamentous structures, in multiple orthogonal planes. There are multiple imaging techniques and pulse sequences for magnetic resonance imaging of the knee. The purposes of this report are to update orthopaedic surgeons on the applications of and indications for magnetic resonance imaging of the knee, define the normal anatomy of the knee as seen on magnetic resonance imaging, and illustrate the spectrum of disease detectable by magnetic resonance imaging.

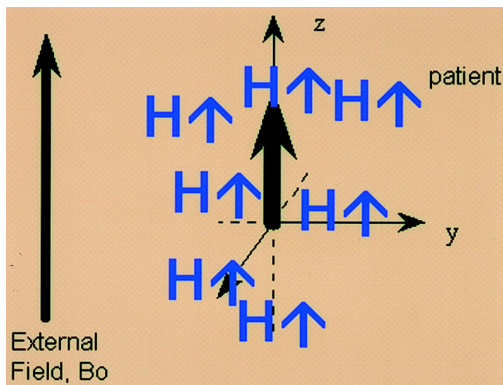


Fig. 1

Diagram showing alignment of the protons within a patient with the external magnetic field (B_0) applied by the superconducting magnet in a typical magnetic resonance imaging scanner.

Educational Objectives

After reviewing this article, the reader should (1) have a basic understanding of the physics, pulse sequences, and terminology of magnetic resonance imaging; (2) be able to systematically evaluate a complete magnetic resonance imaging examination of the knee and know the features of normal knee anatomy; (3) be able to identify various tissue types on T1-weighted, T2-weighted, and fat-suppressed T2-weighted images; (4) be able to develop a differential diagnosis when a patient has knee pain; and (5) be able to review a series of cases and decide whether magnetic resonance imaging is indicated and be able to provide a diagnosis after evaluating the images.

Essentials of Magnetic Resonance Imaging

Process of image production (Figs. 1 through 4): After the patient is placed in the scanner, the magnetic field of the scanner (often 1.5 T) aligns all protons within the patient along the longitudinal axis of the scanner. An electromagnetic pulse is sent into the scanner and causes reorientation of the protons (usually 90° to the external field). The pulse is turned off, and the protons are allowed to relax. As the pro-

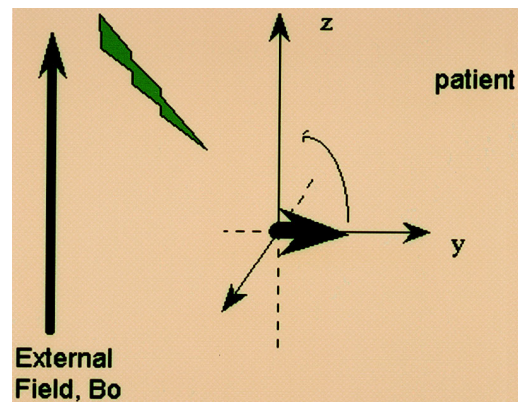


Fig. 2

Diagram showing the application of a radiofrequency pulse to the patient, which often aligns the net magnetization vector of the patient at a 90° angle to the external magnetic field.

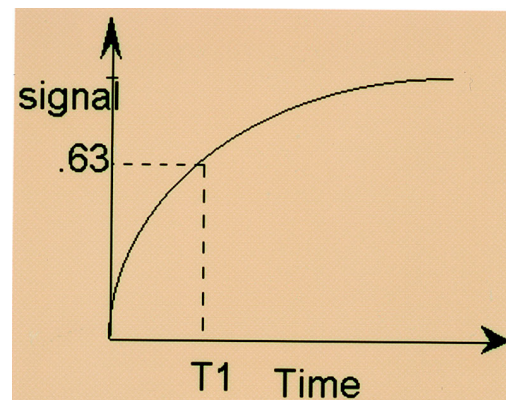


Fig. 3

Graph showing the longitudinal relaxation of the protons, which is measured to determine the characteristics of a tissue on a T1-weighted image.

TABLE I Basic Pulse Sequences for Magnetic Resonance Imaging

Image Type	Repetition Time	Echo Time	Signal Intensity		Advantages	Disadvantages
			Fat	Water		
T1-weighted	Short	Short	Bright	Dark	Best anatomic detail, rapid acquisition	Poor demonstration of pathology/edema
T2-weighted	Long	Long	Intermediate	Bright	Moderately sensitive for pathology/edema	Poor spatial resolution, time-consuming
Fat-suppressed T2-weighted	Long	Short	Very dark	Very bright	Most sensitive for pathology/edema	Poor spatial resolution, time-consuming
Gradient echo	Short	Short	Intermediate	Intermediate/high	Excellent for evaluation of articular cartilage, pigmented villonodular synovitis, and blood	Very susceptible to metallic artifacts (prostheses)
Proton density	Long	Short	Intermediate/high	Intermediate	Excellent for evaluation of meniscal pathology	

tons relax, they emit a radiofrequency signal that is picked up by an antenna in the scanner. The signal is processed by the computer (Fourier transformation), and software programs are used to create the images in multiple orthogonal planes.



Fig. 4
Sagittal T1-weighted image, the result of the process shown in Figs. 1, 2, and 3.

Definitions: T1 indicates the amount of time required for 63% of the protons to return to their preexcited state. It is a measure of the longitudinal relaxation of protons. T2 indicates the amount of

time required for 63% of the protons to “dephase”—that is, to start processing at frequencies different from the applied electromagnetic pulse. It is a measure of the transverse relaxation of protons.

Types of pulse sequences: By manipulating the strength of a radiofrequency pulse, how frequently it is sent in, and how long after the pulse the energy emitted by relaxation is measured, the images can be weighted to emphasize the T1, T2, or proton-density characteristics of a tissue (Table I). A T1-weighted image



Fig. 5
Coronal T1-weighted image showing excellent anatomic detail.

(Fig. 5) has the highest resolution and is the best choice for determining anatomy. A T2-weighted image (Fig. 6) is often noisy looking, has a lower resolution, is susceptible to motion artifact, and is sensitive to pathological changes in tissue, including any process in which cells and the extracellular matrix have an increased water content. To obtain a fat-suppressed T2-weighted (STIR) image (Fig. 7), a T2-weighted image is acquired



Fig. 6
Sagittal T2-weighted image showing high-signal-intensity fluid within the knee joint and a tear of the posterior cruciate ligament (arrow).

with a pulse sequence to suppress fat and to accentuate fluid and edema. This pulse sequence is the most sensitive to pathological change and edema. A proton-

TABLE II Tissue Characteristics on Magnetic Resonance Imaging

Tissue Type	Signal Intensity				
	T1-Weighted Image	T2-Weighted Image	Fat-Suppressed T2-Weighted Image	Gradient-Echo Image	Proton-Density Image
Cortical bone	Very low	Very low	Very low	Very low	Very low
Yellow marrow	High	Intermediate	Very low	Low	Intermediate
Red marrow	Low/intermediate	Intermediate	Low/intermediate	Intermediate	Intermediate/high
Fat	High	Intermediate	Low/intermediate	Intermediate/high	Intermediate/high
Fluid	Low	High	Very high	Intermediate	Low
Muscle	Intermediate	Intermediate	Low/intermediate	Intermediate	Low
Ligaments/tendons	Low	Low	Very low	Very low	Very low
Hyaline cartilage	Intermediate	Intermediate	Intermediate	Intermediate/high	Intermediate
Physeal scar	Low	Low	Low	Low	Low
Meniscus	Low	Low	Low	Low	Low

density image (Fig. 8), which is intermediate between T1-weighted and T2-weighted images, is considered by many to be the sequence of choice for evaluation of the menisci. It is also used for evaluation of articular cartilage. A gradient-echo image



Fig. 7
Coronal fat-suppressed T2-weighted image showing increased signal at the lateral tibial plateau and the lateral aspect of the medial femoral condyle in a patient with an anterior cruciate ligament tear.

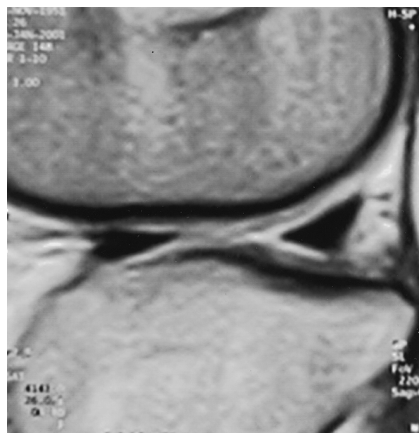


Fig. 8
A sagittal proton-density image allows optimal evaluation of the menisci.

(Fig. 9) is another pulse sequence that is intermediate between T1-weighted and T2-weighted images. It is often used for the evaluation of articular cartilage and is also excellent for the assessment of hemorrhage and pigmented villonodular synovitis, both of which produce signal dropout.



Fig. 9
An axial gradient-echo image allows optimal evaluation of the articular cartilage.

Pulse Sequences and Tissue Characterization

The basic steps in image interpretation include the following.

1. Determine the pulse sequence (Tables I and II).
2. Look for normal anatomy on T1-weighted, proton-density, and gradient-echo images and evaluate for the presence of abnormal structures.
3. Confirm that all tissues are homogeneous on T1-weighted images. If they are not, check T2-weighted images to verify abnormality.
4. Evaluate T2-weighted images for areas of increased signal, which is sensitive, but not specific, for pathology.
5. Correlate magnetic resonance imaging findings with clinical history to determine the most likely diagnosis.



Fig. 10

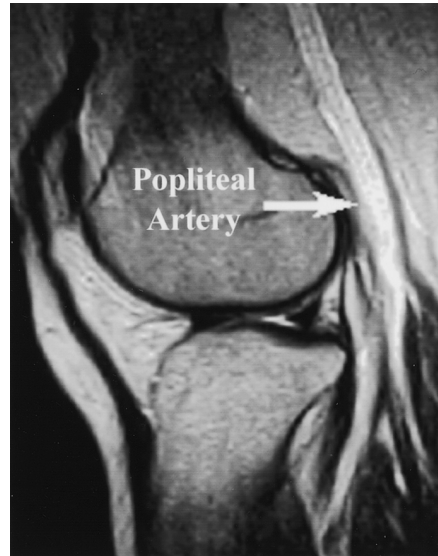


Fig. 11

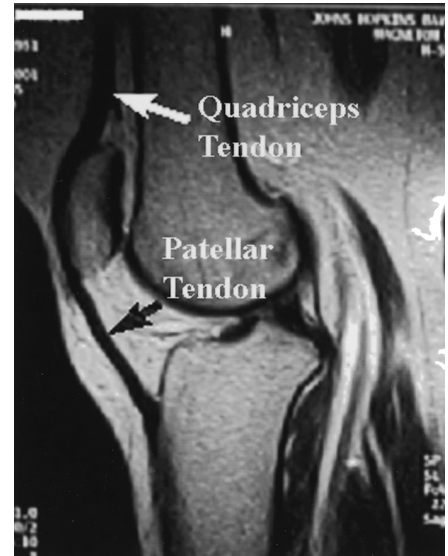


Fig. 12



Fig. 13



Fig. 14



Fig. 15

Figs. 10 through 15 Sagittal T2-weighted images showing normal anatomy of the knee from lateral (Fig. 10) to medial (Fig. 15). ACL = anterior cruciate ligament, and PCL = posterior cruciate ligament.

Normal Anatomy of the Knee as Seen on Magnetic Resonance Imaging Sagittal Images (Figs. 10 through 15)

Sagittal images are best used to evaluate the anterior and posterior cruciate ligaments. They also provide excellent visualization of the menisci. The extensor mechanism, including the quadriceps and patellar tendons, and the patellofemoral joint are well visualized on midsagittal images. Each sagittal image should be evaluated systematically, from one side of the knee to the other. Note that the lateral compartment is identified by the presence of the fibular head as well as a convex contour of the tibial plateau. The medial compartment characteristically has a concave tibial contour. Also, when images

are viewed from lateral to medial, the anterior cruciate ligament is seen before the posterior cruciate ligament¹.

Anterior cruciate ligament: This ligament extends obliquely from the posteromedial aspect of the lateral femoral condyle to its insertion site 15 mm posterior to the anterior border of the tibial articular surface. The anterior cruciate ligament is usually seen on at least one sagittal image when 5-mm-thick sections are used. Note that it is not as well defined as the posterior cruciate ligament; this is a normal finding. Also, the fibers of the anterior cruciate ligament usually display a higher signal intensity than those of the posterior cruciate ligament.

Posterior cruciate ligament: This ligament shows a thick

and uniformly low signal intensity. It extends from the anterolateral aspect of the medial femoral condyle to the posteroinferior tibial surface. The anterior meniscomfemoral ligament (ligament of Humphry) and the posterior meniscomfemoral ligament (ligament of Wrisberg) can be seen in association with the posterior cruciate ligament.

Menisci: Menisci show uniformly low signal intensity. The body of the medial meniscus has a bow-tie shape on at least one or two sagittal images. The meniscal horns appear as opposing triangles on at least two or three consecutive images that approach the intercondylar notch.

Other structures: The quadriceps and patellar tendons are best seen on midsagittal images and show a uniformly low signal. Hoffa's infrapatellar fat pad is seen just posterior to the patellar tendon and follows the signal of subcutaneous fat on all pulse sequences. The popliteal vessels are well visualized, with the popliteal artery anterior to the vein.

Coronal Images

(Figs. 16 through 19)

Coronal images are best used to evaluate the collateral ligament anatomy. These images also show the femoral condyles and can be used to correlate findings with those seen on sagittal images. Although the cruciate ligaments are best seen on sagittal images, they can also be identified on coronal images. Coronal images may also be used to evaluate the popliteus tendon and the femorotibial joint. Coronal images should be followed from the posterior structures, including the popliteal vessels and the posterior aspect of the femoral condyles, to the anterior structures, including the extensor mechanism.

Collateral ligaments: The normal medial collateral ligament is 8 to 10 cm long and is seen as a uniformly low-signal-intensity line extending from its attachment on the medial femoral epicondyle to the medial aspect of the proximal part of the tibia, approximately 5 to 7 cm distal to the tibial plateau, deep to the pes anserinus insertion. The major contributors to the lateral collateral ligament complex are the iliotibial band,

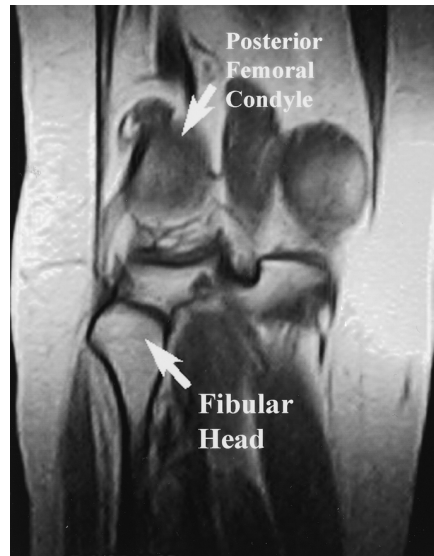


Fig. 16

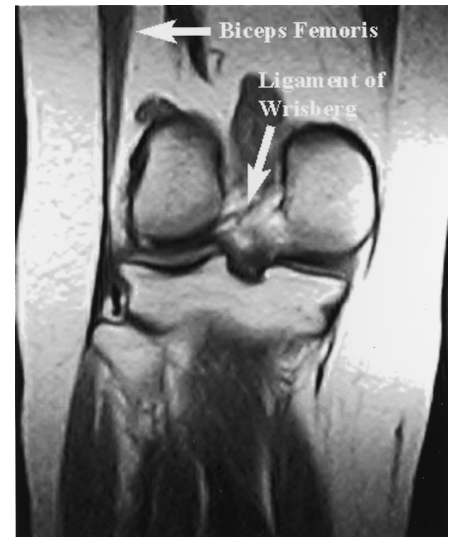


Fig. 17



Fig. 18

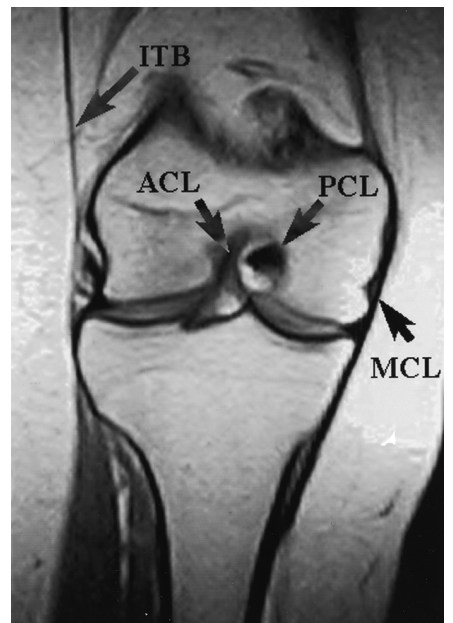


Fig. 19

Figs. 16 through 19 Coronal T1-weighted images showing normal anatomy of the knee from posterior (Fig. 16) to anterior (Fig. 19). LCL = lateral collateral ligament, ITB = iliotibial band, ACL = anterior cruciate ligament, PCL = posterior cruciate ligament, and MCL = medial collateral ligament.

the fibular (lateral) collateral ligament, and the biceps femoris tendon. The iliotibial band is seen on multiple anterior images and inserts onto Gerdy's tubercle on the anterolateral aspect of the tibial plateau. The lateral collateral ligament extends from the lateral femoral condyle to the fibular head.

Anterior and posterior cruciate ligaments: The anterior cruciate ligament

is oriented more vertically relative to the posterior cruciate ligament in the intercondylar notch. The insertion of the anterior cruciate ligament onto the lateral aspect of the medial tibial spine is well seen on the anterior images. The posterior cruciate ligament has a triangular appearance on posterior coronal images and a more circular appearance on anterior images.

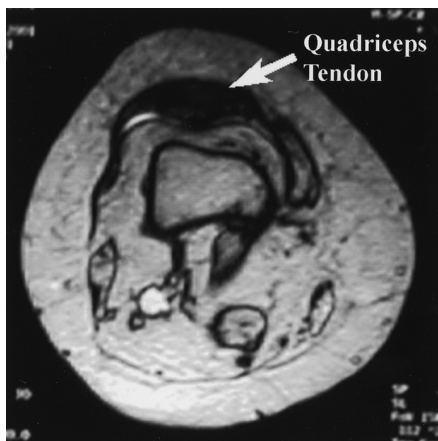


Fig. 20

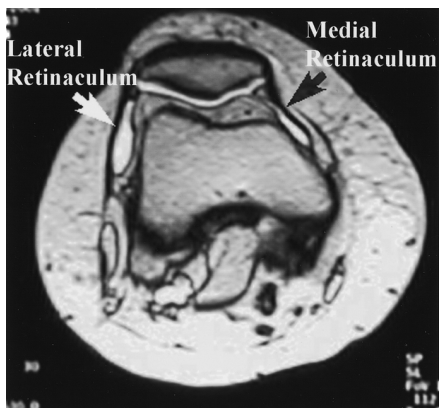


Fig. 21

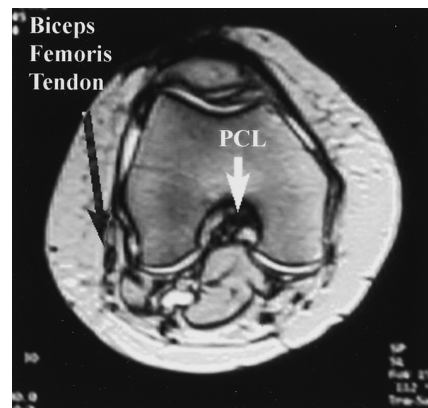


Fig. 22

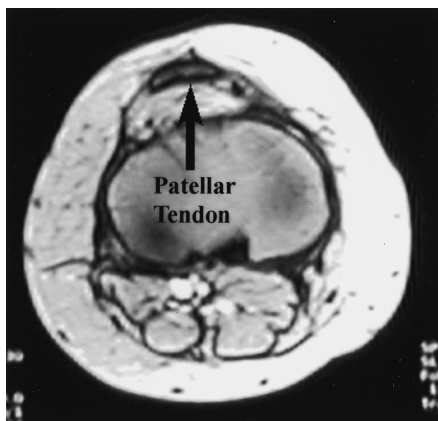


Fig. 23

Figs. 20 through 23 Axial T2-weighted images showing normal anatomy of the knee from proximal (Fig. 20) to distal (Fig. 23). PCL = posterior cruciate ligament.

groove. The relationship of the patella to the trochlea, including patellar tilt and subluxation, is best assessed on these images. Axial images provide excellent visualization of the patellar retinacula and can be used as a secondary plane for confirming or ruling out patellar and quadriceps tendon pathology seen on sagittal images and collateral ligament injuries seen on coronal images. Note that the anterior cruciate ligament is seen coursing in a 15° to 20° anteromedial direction in the intercondylar notch from the medial aspect of the lateral femoral condyle to the anterior aspect of the tibia. The posterior cruciate ligament originates from the lateral aspect of the medial femoral

condyle and is triangular or circular in cross section.

Evaluation of Knee Pathology

Normal Menisci (Figs. 24 through 27)

Multiple pulse sequences have been ad-

Axial Images (Figs. 20 through 23)

Axial images are best used to evaluate the articular cartilage of the medial and lateral patellar facets and the trochlear

Figs. 24 through 27 Sagittal proton-density images showing normal meniscal anatomy from lateral (Fig. 24) to medial (Fig. 27). ACL = anterior cruciate ligament, and PCL = posterior cruciate ligament.

Fig. 24

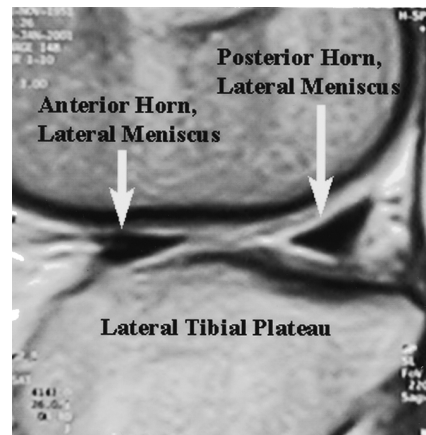


Fig. 27

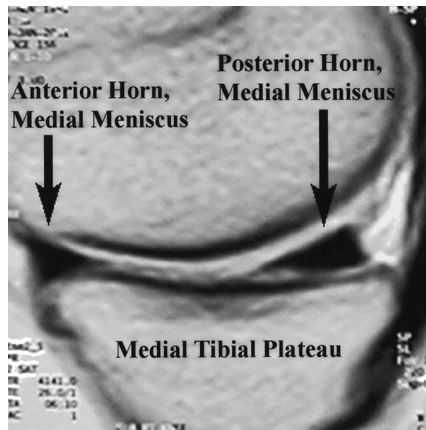


Fig. 25

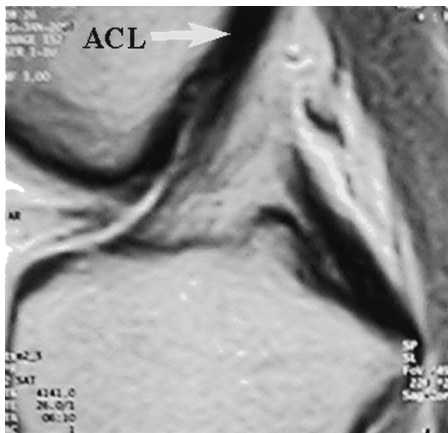


Fig. 26

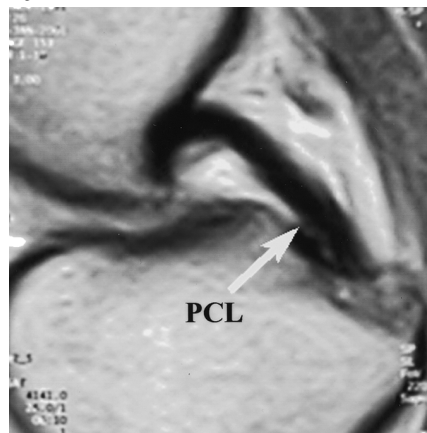


TABLE III Characteristics of Meniscal Tears on Magnetic Resonance Imaging

Tear Type	Description	Findings on Magnetic Resonance Imaging
Horizontal	Separates meniscus into superior (femoral) and inferior (tibial) fragments	Primarily horizontal signal on sagittal images
Vertical	Separates meniscus into anterior and posterior fragments	Primarily vertical signal on sagittal images
Longitudinal	Extends along length of meniscus; separates meniscus into inner and outer fragments	Tear location remains same distance from outer margin on sequential images
Radial	Vertical tear perpendicular to free edge of meniscus	Vertical hyperintensity on sagittal images
Oblique	Traverses meniscus obliquely	As tear is traced on sequential images, moves closer to inner margin of meniscus
Bucket-handle	Subtype of longitudinal tear in which displaced central fragment resembles a bucket handle	"Double posterior cruciate ligament sign"; displaced fragment often seen parallel to posterior cruciate ligament in intercondylar notch on sagittal images
Complex	Combination of multiple planes; commonly horizontal and radial	Characteristics of each tear type or fragmented/macerated

TABLE IV Grading of Meniscal Tears

Grade	Pathological and Magnetic Resonance Imaging Findings
1	Degenerative process; focal, globular intrasubstance increased signal; no extension to articular surface
2	Degenerative process; horizontal, linear intrasubstance increased signal; no extension to articular surface
3	Meniscal tear; increased signal extends to or communicates with at least one articular surface
4	Complex tear/macerated meniscus

Meniscal Tears (Figs. 28 through 34)

The primary use of magnetic resonance imaging of the menisci is to define and characterize meniscal tears (Tables III and IV).

Ligaments

Anterior cruciate ligament (Figs. 7 and 35): Evaluation of the anterior cruciate ligament is one of the primary indications for magnetic resonance imaging of the knee. It is important to know the primary and secondary signs of an anterior cruciate tear (Table V)¹⁰⁻¹⁴.

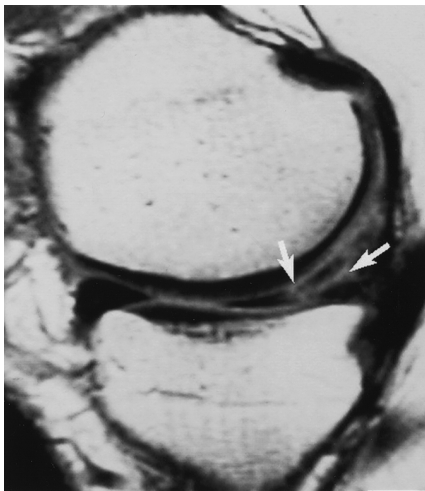


Fig. 28
Sagittal proton-density image showing a complex tear of the posterior horn of the medial meniscus (arrows).

vocated for meniscal imaging. At our institution, meniscal evaluation is performed primarily with proton-density images. Tears can also be seen well on T1-weighted images and gradient-echo images. In general, T2-weighted images are less sensitive in detecting meniscal

tears. The normal meniscus shows low signal intensity on all pulse sequences.



Fig. 29
Sagittal proton-density image showing a grade-2 tear of the posterior horn of the lateral meniscus.

The menisci should be evaluated on all sagittal images²⁻⁹.

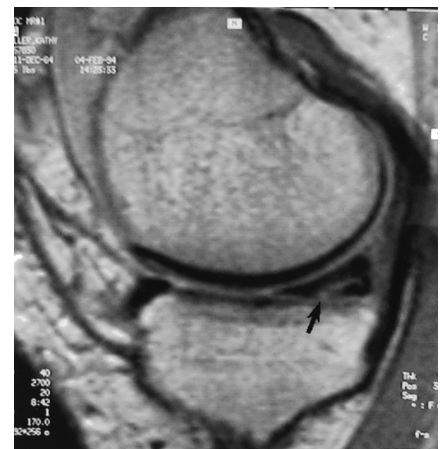


Fig. 30
Sagittal proton-density image showing a grade-3 tear of the posterior horn of the medial meniscus (arrow).



Fig. 31
Sagittal proton-density image showing a radial tear of the lateral meniscus (arrow).



Fig. 34
Coronal fat-suppressed T2-weighted image showing a lateral meniscal cyst (arrow).



Fig. 36
Sagittal T2-weighted image showing a tear of the posterior cruciate ligament (arrow) at its tibial attachment.



Fig. 32
Sagittal T1-weighted image showing the "double posterior cruciate ligament sign" (arrow), which is commonly seen with bucket-handle meniscal tears.



Fig. 35
Sagittal T1-weighted image showing a tear of the anterior cruciate ligament (arrow).



Fig. 37
Sagittal T2-weighted image showing a tear in the midsubstance of the posterior cruciate ligament (arrow).

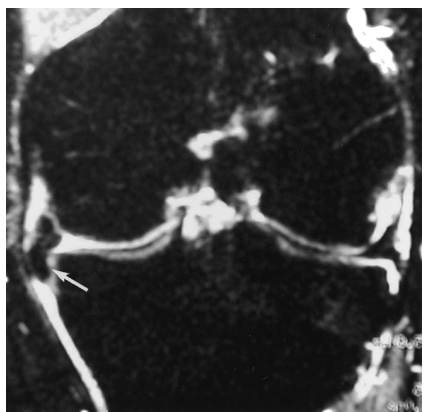


Fig. 33
Coronal fat-suppressed T2-weighted image showing a displaced tear of the medial meniscus with the meniscal fragment (arrow) interposed between the joint line and the medial collateral ligament.

Fig. 38
Coronal fat-suppressed T2-weighted image showing a grade-I tear of the medial collateral ligament (arrow).

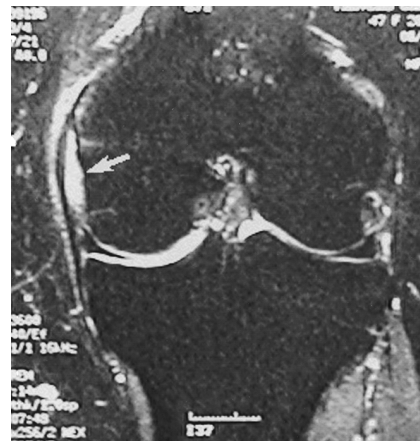


TABLE V Anterior Cruciate Ligament Tears

Primary Signs of Tear

- Nonvisualization of ligament
- Complete disruption of a ligament segment
- Abnormal signal within ligament
- Alteration of normal linear configuration of ligament
- Alteration of normal ligament orientation nearly parallel or at acute angle to notch roof

Secondary Signs of Tear

- Bone contusions
- Deepening of lateral femoral condyle notch or sulcus
- Anterior translation of tibia >5 mm from posterior margin of femoral condyle
- Buckling of posterior cruciate ligament
- Posterior displacement of posterior horn of lateral meniscus

Posterior cruciate ligament (Figs. 36 and 37): The posterior cruciate ligament is seen well on sagittal T1-weighted and T2-weighted images. Magnetic resonance imaging allows evaluation of both sprains and tears of the posterior cruciate ligament¹⁵⁻¹⁷.



Fig. 39



Fig. 40

Fig. 39 Coronal T1-weighted image suggesting an injury of the medial collateral ligament. **Fig. 40** Coronal fat-suppressed T2-weighted image of the same patient as in Fig. 39, showing a grade-II tear of the medial collateral ligament.

Collateral ligaments (Figs. 38 through 41): The collateral ligaments are best seen on coronal T1-weighted and T2-weighted images. Increased signal intensity on T2-weighted images is compatible with edema and indicates the acuity of the injury. T1-weighted images can be used to follow the contour of the ligaments and to differentiate a ligamentous sprain from a complete (grade-III) tear (Table VI).

TABLE VI Collateral Ligament Tears

Grade	Pathological Findings
I	Periligamentous edema; ligament grossly intact
II	Partial tear with edema
III	Complete tear

Fig. 41 Coronal fat-suppressed T2-weighted image showing a grade-III tear of the medial collateral ligament (arrow). **Fig. 42** Sagittal T2-weighted image showing increased signal within the patellar tendon compatible with patellar tendinitis (arrow). **Fig. 43** Sagittal T2-weighted image showing complete disruption of the quadriceps tendon at its patellar insertion site (arrow).

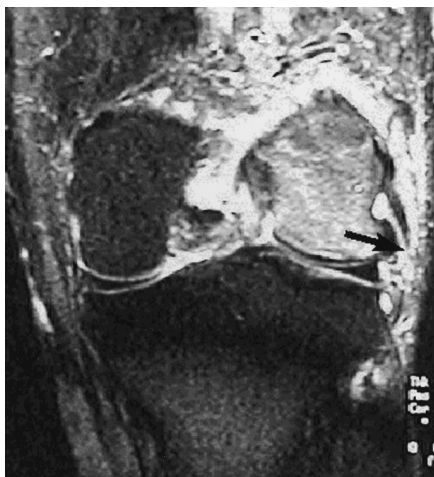


Fig. 41



Fig. 42

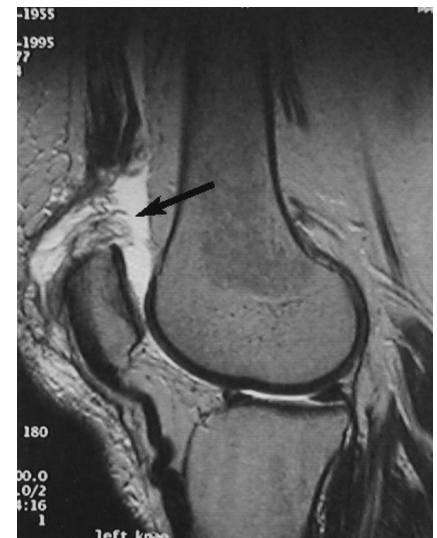


Fig. 43



Fig. 44

Sagittal fat-suppressed gradient-echo image showing the normal femoral articular cartilage (arrows).

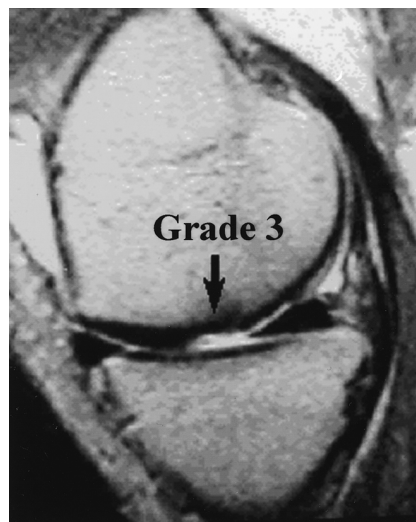


Fig. 45

Sagittal proton-density image showing grade-3 chondromalacia of the femoral articular cartilage (arrow).

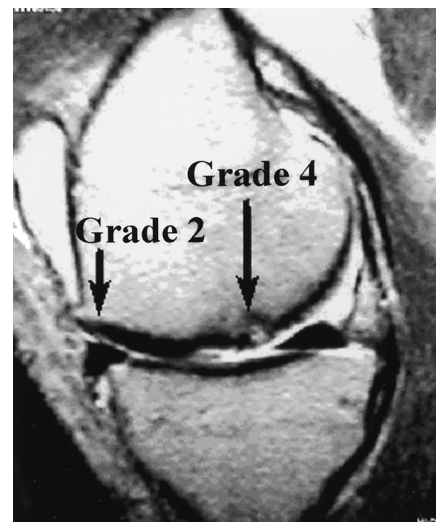


Fig. 46

Sagittal proton-density image showing grade-2 and grade-4 chondromalacia of the femoral articular cartilage (arrows).

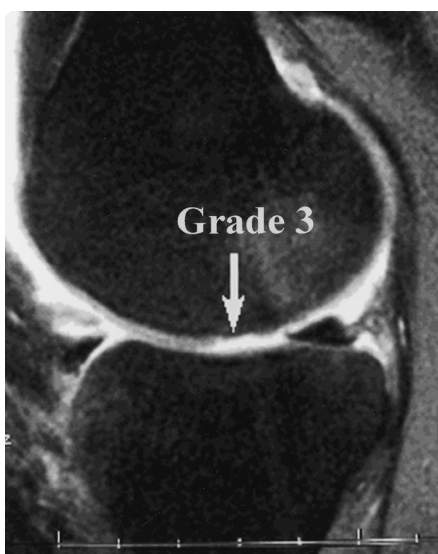


Fig. 47

Sagittal fat-suppressed gradient-echo image showing grade-3 chondromalacia of the femoral articular cartilage (arrow).

Extensor mechanism (Figs. 42 and 43)

The extensor mechanism consists of the quadriceps tendon, the patella, and the patellar tendon. Tendinitis and rupture of the quadriceps and patellar tendons are demonstrated well on sagittal images¹⁸⁻²¹.

Cartilage (Figs. 44 through 51)

Magnetic resonance imaging of cartilage remains a challenge. There is no uni-

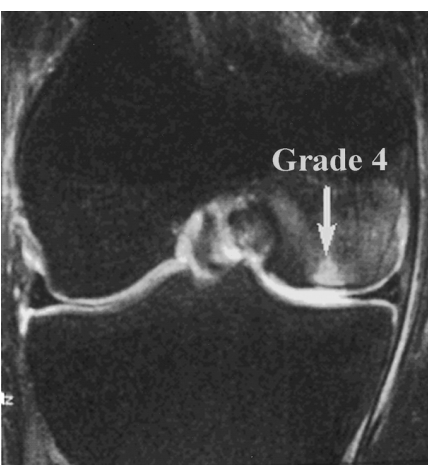


Fig. 48

Coronal fat-suppressed gradient-echo image showing grade-4 chondromalacia of the femoral articular cartilage (arrow).



Fig. 49

Axial fat-suppressed gradient-echo image showing grade-2 chondromalacia of the patellar articular cartilage (arrow).

form consensus regarding the optimal pulse sequence for cartilage imaging. Magnetic resonance imaging generally tends to underestimate the degree of cartilage abnormalities seen with arthroscopy. The two types of pulse sequences currently considered to be the most effective are fat-suppressed fast-spin-echo proton-density and gradient-echo imaging. The degree of chondromalacia can be graded (Table VII). Although the grading system was originally developed for arthroscopic evaluation, it can be

TABLE VII Grading of Chondromalacia

Grade	Pathological Findings
0	Normal cartilage
1	Fibrillation
2	Superficial pitting
3	Nearly complete cartilage loss to level of subchondral bone
4	Complete cartilage loss; exposed subchondral bone



Fig. 50

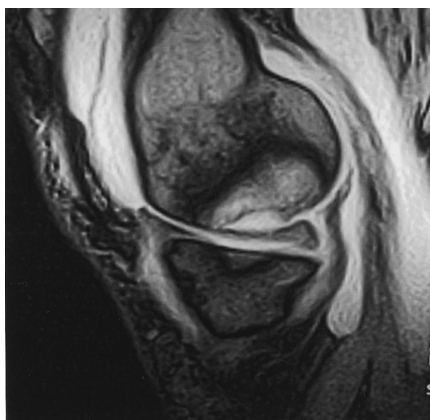


Fig. 51

Fig. 50 Coronal T2-weighted image showing an osteochondritis dissecans lesion of the medial femoral condyle. **Fig. 51** Sagittal T2-weighted image of the same patient as in Fig. 50, showing an osteochondritis dissecans lesion of the medial femoral condyle.

TABLE VIII Osteonecrosis

Parameter	Spontaneous Osteonecrosis of the Knee	Atraumatic Osteonecrosis of the Knee
Synonyms	SPONK, SONK	Secondary or steroid-associated osteonecrosis
Location	Medial femoral condyle	Multiple condyles, tibial involvement in 20% to 30%
Distribution	Subcortical	Epiphyseal, metaphyseal, and diaphyseal common
Age of patients	Usually >60 yr	Usually <45 yr
Bilateral knee involvement	<1%	>80%
Hip involvement	None	90%
Associated risk factors	Rare	>80% (e.g., steroids, alcohol)
Pathogenesis	May represent microtrauma, osteoarthritis, or osteopenia	Multiple theories regarding etiology

applied to magnetic resonance images, albeit with less accuracy²²⁻²⁸.

Osteonecrosis (Figs. 52 through 56)
Magnetic resonance imaging aids in the differentiation of spontaneous osteone-

crosis of the knee from atraumatic osteonecrosis of the knee (Table VIII)²⁹.

Tumors (Figs. 57 through 60)
Benign and malignant bone and soft-tissue tumors are occasionally found on



Fig. 52



Fig. 53



Fig. 54

Fig. 52 Coronal T1-weighted image showing spontaneous osteonecrosis of the knee

involving the femoral condyle (arrow). **Fig. 53** Coronal fat-suppressed T2-weighted image showing the same spontaneous osteonecrosis lesion of the knee (arrow) as in Fig. 52. **Fig. 54** Sagittal proton-density image showing the same spontaneous osteonecrosis lesion of the knee (arrows) as in Figs. 52 and 53.



Fig. 55

Coronal fat-suppressed T2-weighted image showing atraumatic osteonecrosis of the femur and the tibia.



Fig. 56

Sagittal fat-suppressed T2-weighted image showing atraumatic osteonecrosis of the femur and the tibia.

routine magnetic resonance imaging of the knee. These lesions most often show low signal intensity on T1-weighted images and heterogeneously high signal intensity on T2-weighted images. Many bone tumors are better evaluated on conventional radiographs, and magnetic resonance imaging is often used to define the extent of involvement and



Fig. 57

Coronal T1-weighted image showing a lobulated mass infiltrating the distal part of the femur. This lesion shows indeterminate characteristics on magnetic resonance imaging and requires additional evaluation, including a possible biopsy, for a definite diagnosis.



Fig. 58

Sagittal fat-suppressed T2-weighted image showing the same mass as in Fig. 57.

the intracompartmental or extracompartmental nature of the tumor. Magnetic resonance imaging is most useful for the evaluation of soft-tissue tumors about the knee. It allows classification of a soft-tissue tumor as either determinate or indeterminate. Determinate lesions are processes that can be assigned a diagnosis, with a high level of confidence, with the use of magnetic reso-



Fig. 59

Sagittal gradient-echo image showing multiple small lesions (arrows), which demonstrate signal dropout, within the knee joint. This appearance of the magnetic resonance image is compatible with pigmented villonodular synovitis.



Fig. 60

Sagittal gradient-echo image of the same patient in Fig. 59, showing a collection of pigmented villonodular synovitis nodules in the popliteal fossa (arrows).

TABLE IX Soft-Tissue Tumors

Determinate Lesions	Characteristics on Magnetic Resonance Imaging
Lipoma	Follow fat signal on all pulse sequences, including fat-suppressed sequences
Ganglion cyst/Baker's cyst	Low signal intensity on T1-weighted images, high signal intensity on T2-weighted images, well circumscribed, communicates with joint
Hemangioma	Soft-tissue mass with serpentine regions of signal void shown equally well on T1-weighted and T2-weighted images
Bursitis	Low signal intensity on T1-weighted images, high signal intensity on T2-weighted images, often well circumscribed and in the region of a bursa, often draped over a tendon
Muscle tears/tendon ruptures	T1-weighted images demonstrate muscular or tendinous deformity, T2-weighted images show high signal intensity compatible with surrounding edema and hemorrhage
Pigmented villonodular synovitis	Substantially decreased or absent signal on both T1-weighted and T2-weighted images, profound signal dropout on gradient-echo images, often a heterogeneous synovial process extending away from knee joint
Neurofibroma	Soft-tissue mass in perineural location, homogeneous on T1-weighted images with signal intensity slightly greater than that of muscle, T2-weighted images show "target sign" with a central region of low signal intensity

nance imaging (Table IX). Indeterminate lesions require further evaluation, usually with needle or incisional biopsy³⁰. ■

A. Jay Khanna, MD
Andrew J. Cosgarea, MD
Brett M. Andres, MD
David A. Bluemke, MD, PhD
Frank J. Frassica, MD

Departments of Orthopaedic Surgery (A.J.K., A.J.C., B.M.A., and F.J.F.) and Radiology (D.A.B.), The Johns Hopkins Hospital, 601 North Caroline Street, Baltimore, MD 21287-0882. Please address correspondence and reprint requests to Frank J. Frassica, MD, c/o Elaine P. Bulson, Medical Editor, Department of Orthopaedic Surgery, Johns Hopkins Bayview Medical Center, 4940 Eastern Avenue, Baltimore, MD 21224-2780

Michael A. Mont, MD
Sinai Hospital, Belvedere and Greenspring, Baltimore, MD 21215

Benjamin G. Domb, MD
Hospital for Special Surgery, 535 East 70th Street, New York, NY 10021

Peter J. Evans, MD
The Cleveland Clinic, 9500 Euclid Avenue, Cleveland, OH 44195

The authors did not receive grants or outside funding in support of their research or preparation of this manuscript. They did not receive payments or other benefits or a commitment or agreement to provide such benefits from a commercial entity. No commercial entity paid or directed, or agreed to pay or direct, any benefits to any research fund, foundation, educational institution, or other charitable or nonprofit organization with which the authors are affiliated or associated.

References

1. **Stoller DW.** *Magnetic resonance imaging in orthopaedics and sports medicine.* 2nd ed. Philadelphia: Lippincott-Raven; 1997.
2. **Cheung LP, Li KC, Hollett MD, Bergman AG, Herfkens RJ.** Meniscal tears of the knee: accuracy of detection with fast spin-echo MR imaging and arthroscopic correlation in 293 patients. *Radiology.* 1997;203:508-12.
3. **Deutsch AL, Mink JH, Fox JM, Arnoczky SP, Rothman BJ, Stoller DW, Cannon WD Jr.** Peripheral meniscal tears: MR findings after conservative treatment or arthroscopic repair. *Radiology.* 1990;176:485-8.
4. **Justice WW, Quinn SF.** Error patterns in the MR imaging evaluation of menisci of the knee. *Radiology.* 1995;196:617-21.
5. **Kaplan PA, Nelson NL, Garvin KL, Brown DE.** MR of the knee: the significance of high signal in the meniscus that does not clearly extend to the surface. *AJR Am J Roentgenol.* 1991;156:333-6.
6. **Kornick J, Trefelner E, McCarthy S, Lange R, Lynch K, Joki P.** Meniscal abnormalities in the asymptomatic population at MR imaging. *Radiology.* 1990;177:463-5.
7. **Rubin DA, Paletta GA Jr.** Current concepts and controversies in meniscal imaging. *Magn Reson Imaging Clin N Am.* 2000;8:243-70.
8. **Stoller DW, Martin C, Crues JV 3rd, Kaplan L, Mink JH.** Meniscal tears: pathologic correlation with MR imaging. *Radiology.* 1987;163:731-5.
9. **Wright DH, De Smet AA, Norris M.** Bucket-handle tears of the medial and lateral menisci of the knee: value of MR imaging in detecting displaced fragments. *AJR Am J Roentgenol.* 1995;165:621-5.
10. **Gentili A, Seeger LL, Yao L, Do HM.** Anterior cruciate ligament tear: indirect signs at MR imaging. *Radiology.* 1994;193:835-40.
11. **Graf BK, Cook DA, De Smet AA, Keene JS.** "Bone bruises" on magnetic resonance imaging evaluation of anterior cruciate ligament injuries. *Am J Sports Med.* 1993;21:220-3.
12. **Robertson PL, Schweitzer ME, Bartolozzi AR, Ugoni A.** Anterior cruciate ligament tears: evaluation of multiple signs with MR imaging. *Radiology.* 1994;193:829-34.
13. **Tung GA, Davis LM, Wiggins ME, Fadale PD.** Tears of the anterior cruciate ligament: primary and secondary signs at MR imaging. *Radiology.* 1993;188:661-7.
14. **Umans H, Wimpfheimer O, Haramati N, Applbaum YH, Adler M, Bosco J.** Diagnosis of partial tears of the anterior cruciate ligament of the knee: value of MR imaging. *AJR Am J Roentgenol.* 1995;165:893-7.
15. **Gross ML, Grover JS, Bassett LW, Seeger LL, Finerman GA.** Magnetic resonance imaging of the posterior cruciate ligament. Clinical use to improve diagnostic accuracy. *Am J Sports Med.* 1992;20:732-7.
16. **Sonin AH, Fitzgerald SW, Friedman H, Hoff FL, Hendrix RW, Rogers LF.** Posterior cruciate ligament injury: MR imaging diagnosis and patterns of injury. *Radiology.* 1994;190:455-8.

17. **Sonin AH, Fitzgerald SW, Hoff FL, Friedman H, Bresler ME.** MR imaging of the posterior cruciate ligament: normal, abnormal, and associated injury patterns. *Radiographics*. 1995;15:551-61.
18. **Sonin AH, Fitzgerald SW, Bresler ME, Kirsch MD, Hoff FL, Friedman H.** MR imaging appearance of the extensor mechanism of the knee: functional anatomy and injury patterns. *Radiographics*. 1995;15:367-82.
19. **Yu JS, Petersilge C, Sartoris DJ, Pathria MN, Resnick D.** MR imaging of injuries of the extensor mechanism of the knee. *Radiographics*. 1994;14:541-51.
20. **Yu JS, Popp JE, Kaeding CC, Lucas J.** Correlation of MR imaging and pathologic findings in athletes undergoing surgery for chronic patellar tendinitis. *AJR Am J Roentgenol*. 1995;165:115-8.
21. **Zeiss J, Saddemi SR, Ebraheim NA.** MR imaging of the quadriceps tendon: normal layered configuration and its importance in cases of tendon rupture. *AJR Am J Roentgenol*. 1992;159:1031-4.
22. **Bredella MA, Tirman PF, Peterfy CG, Zarlingo M, Feller JF, Bost FW, Belzer JP, Wischer TK, Genant HK.** Accuracy of T2-weighted fast spin-echo MR imaging with fat saturation in detecting cartilage defects in the knee: comparison with arthroscopy in 130 patients. *AJR Am J Roentgenol*. 1999;172:1073-80.
23. **De Smet AA, Fisher DR, Graf BK, Lange RH.** Osteochondritis dissecans of the knee: value of MR imaging in determining lesion stability and the presence of articular cartilage defects. *AJR Am J Roentgenol*. 1990;155:549-53.
24. **Disler DG, McCauley TR, Kelman CG, Fuchs MD, Ratner LM, Wirth CR, Hospodar PP.** Fat-suppressed three-dimensional spoiled gradient-echo MR imaging of hyaline cartilage defects in the knee: comparison with standard MR imaging and arthroscopy. *AJR Am J Roentgenol*. 1996;167:127-32.
25. **Outerbridge RE.** The etiology of chondromalacia patellae. *J Bone Joint Surg Br*. 1961;43:752-7.
26. **Peterfy CG.** Scratching the surface: articular cartilage disorders in the knee. *Magn Reson Imaging Clin N Am*. 2000;8:409-30.
27. **Potter HG, Linklater JM, Allen AA, Hannafin JA, Haas SB.** Magnetic resonance imaging of articular cartilage in the knee. An evaluation with use of fast-spin-echo imaging. *J Bone Joint Surg Am*. 1998;80:1276-84.
28. **Recht MP, Resnick D.** MR imaging of articular cartilage: current status and future directions. *AJR Am J Roentgenol*. 1994;163:283-90.
29. **Ecker ML, Lotke PA.** Spontaneous osteonecrosis of the knee. *J Am Acad Orthop Surg*. 1994;2:173-8.
30. **Frassica FJ, Khanna JA, McCarthy EF.** The role of MR imaging in soft tissue tumor evaluation: perspective of the orthopaedic oncologist and musculoskeletal pathologist. *Magn Reson Imaging Clin N Am*. 2000;8:915-27.